molbank

MDPI

Short Note

Chlorido-(η^6-*p*-cymene)-(bis(pyrazol-1-yl)methane-κ^2N,N')Osmium(II) Tetrafluoroborate, $C_{17}H_{22}BClF_4N_4Os$

Allen Mambanda [1,*], Amos K. Kanyora [2,*], Peter Ongoma [2], Joel Gichumbi [3] and Reinner O. Omondi [1,4]

jgichumbi@chuka.ac.ke [3]

[1] School of Chemistry and Physics, University of KwaZulu-Natal, Private Bag X01, Scottsville, Pietermaritzburg 3209, South Africa
[2] Department of Chemistry, Egerton University, Egerton P.O. Box 536-20115, Kenya
[3] Department of Physical Sciences, Chuka University, Chuka P.O. Box 109-60400, Kenya
[4] Department of Chemistry, University of Cape Town, Rondebosch 7701, South Africa
* Correspondence: mambanda@ukzn.ac.za (A.M.); kimem.aka12@gmail.com (A.K.K.)

Abstract: The powder of the arene osmium(II) complex, [Os(II)(dpzm)(η^6-*p*-cym)Cl]BF_4 (dpzm = di(1*H*-pyrazol-1-yl)methane; η^6-*p*-cym = *para*-cymene), with a formula of $C_{17}H_{22}BClF_4N_4Os$ (referred to herein as **1**) was isolated from the reaction of [(η^6-*p*-cym)Os(μ-Cl)(Cl)]$_2$ with dpzm dissolved in acetonitrile and under a flow of nitrogen gas. It was characterized by spectroscopic techniques (*viz.*, FTIR, ^{1}H NMR, UV-Visible absorption). Yellow crystal blocks of **1** were grown by the slow evaporation from the methanolic solution of its powder. The single-crystal X-ray structure of **1** was solved by diffraction analysis on a Bruker APEX Duo CCD area detector diffractometer using the Cu(K_α), λ = 1.54178 Å as the radiation source, and **1** crystallizes in the monoclinic crystal system and the C2/c (*no*. 15) space group.

Keywords: arene osmium(II) complex; di(1*H*-pyrazol-1-yl)methane; *para*-cymene; piano stool geometry; pseudo-octahedral geometry

Citation: Mambanda, A.; Kanyora, A.K.; Ongoma, P.; Gichumbi, J.; Omondi, R.O. Chlorido-(η^6-*p*-cymene)-(bis(pyrazol-1-yl)methane-κ^2N,N')Osmium(II) Tetrafluoroborate, $C_{17}H_{22}BClF_4N_4Os$. *Molbank* **2022**, *2022*, M1429. https://doi.org/10.3390/M1429

Academic Editors: Bartolo Gabriele, Raffaella Mancuso and Zhengguo Cai

Received: 18 June 2022
Accepted: 19 July 2022
Published: 18 August 2022

1. Introduction

The acute toxicity, side effects, and development of resistance are some of the disadvantages which have curtailed the widespread uptake and use of current platinum-based chemotherapeutics. This has prompted a continued search for alternatives that have improved efficacies and less physiologically threatening side effects. In addition to Pt(II/IV)complexes, there have been complexes of other metal ions, such as Ti(IV) [1], Au(III) [2], Os(II) [3], Fe(II) [4], and Ru(II) [5], which have been evaluated for their anticancer activities and found to be active. Some of these have shown the potential to overcome the limitations of their platinum(II) counterparts and some have undergone first-phase clinical trials [4].

The element osmium (Os) is a heavier congener of ruthenium (Ru) and shares the same period with platinum. Like ruthenium, it forms stable Os(II)/(III) complexes. Os(III) complexes are thermodynamically stable and kinetically inert. However, under the hyper-acidity and hypoxia conditions of cancer cells, drug designers think that Os(III) complexes can be reduced spontaneously to form the kinetically more labile Os(II) analogues which are thought to be the relevant species for chemotherapy. The lability can be enhanced by the coordination of strong π-accepter ligands on the Os(II) ion. These ligands promote a stronger back-donation of electron density from metal *d*-orbitals of the complexes towards the ligands, thereby increasing the electrophilicity of the metal centre [6,7]. However, compared to Ru(II)'s, Os(II) complexes are expected to have slower ligand exchange kinetics, with rates that should be more comparable to those of Pt(II).

Arenes have been used extensively to stabilize organometallic Ru/Os(II) complexes. They coordinate facially as $6e^-$-π donors to the metal ion. These complexes have the general

formula, [(arene)Ru/Os(II)(Y-/Z)X], where the arene is one of the non-leaving groups and ligates as a $6e^{-}$-π donor ligand. Ligand Y- or /and Z can be a bidentate chelating or two monodentate ligands, while X is a monodentate and good leaving group. They are known as 'half-sandwiches' and usually assume pseudo-octahedral coordination with a "piano-stool" geometry. The other non-leaving ligands of these complexes can be selected carefully to provide an optimum lipophilic–hydrophilic balance to the resultant complex. Both neutral and positively-charged air-stable complexes can be synthesised in moderate to high yields.

The chemotherapeutic applications of Os(II) complexes have not received as much attention as those of Pt(II) or Ru(II). However, some arene Os(II) complexes have been evaluated for their potential as anticancer agents. They have shown high cytotoxic levels, similar to cisplatin's, including in cisplatin-resistant cancer cell lines [8]. These 'piano-stool' complexes have also shown potential as anticancer drugs, with a promising hope of them being alternate anticancer palliatives to the current first to third generation platinum complexes. The coordinated ligands can be tailor-designed to systematically alter the thermodynamic and kinetic properties, apart from the physical properties of the complexes [7]. The cationic complexes are water-soluble, yet they have a hydrophobic arene backbone, and thus exhibit good lipophilicity in lipidic phases, such as the lipo-bilayers of cell membranes [7]. Surprisingly, these complexes are relatively non-toxic. This may be due to the strong M–C bonds that are formed between the potentially toxic arene and the metal ion. The strong bonds prevent the premature release of the arene before the complexes reach their sites for biological activity. Some of the complexes have demonstrated good aqueous solubility and biodistribution in the bloodstream. Their cell membrane permeability is remarkable, and this may explain their unusual high efficacy and selectivity for cancer cells compared to Pt(II) drugs [9]. This paper reports the single-crystal structural data of [Os(II)(dpzm(η^6-*p*-cym)Cl]BF_4 ($C_{17}H_{22}BClF_4N_4Os$), (dpzm = di(1*H*-pyrazol-1-yl)methane, η^6-*p*-cym = *para*-cymene) and its other characterization data collected using various spectral techniques.

2. Results and Discussion

The need for alternative inorganic anticancer agents prompted us to synthesise $C_{17}H_{22}BClF_4N_4Os$ (**1**). The crystal structure of **1** (**cu_am_ro_am_10_5_0m**) was solved by single-crystal X-ray diffraction analysis. The ORTEP representation of the asymmet- ric unit with the atom numbering scheme and cell packing structure of **1** are shown in Figures 1 and 2, respectively.

The crystal data of **1** and its structure refinement details and the selected bond lengths and angles are presented in Tables 1 and 2, respectively. The atomic coordinates ($\times 10^4$) and the equivalent isotropic displacement parameters ($Å^2 \times 10^3$), as well as the bond lengths [Å] and angles [°] for **1** (**cu_am_ro_am_10_5_0m**), are given in Tables S1 and S2, respectively, in the supplementary information.

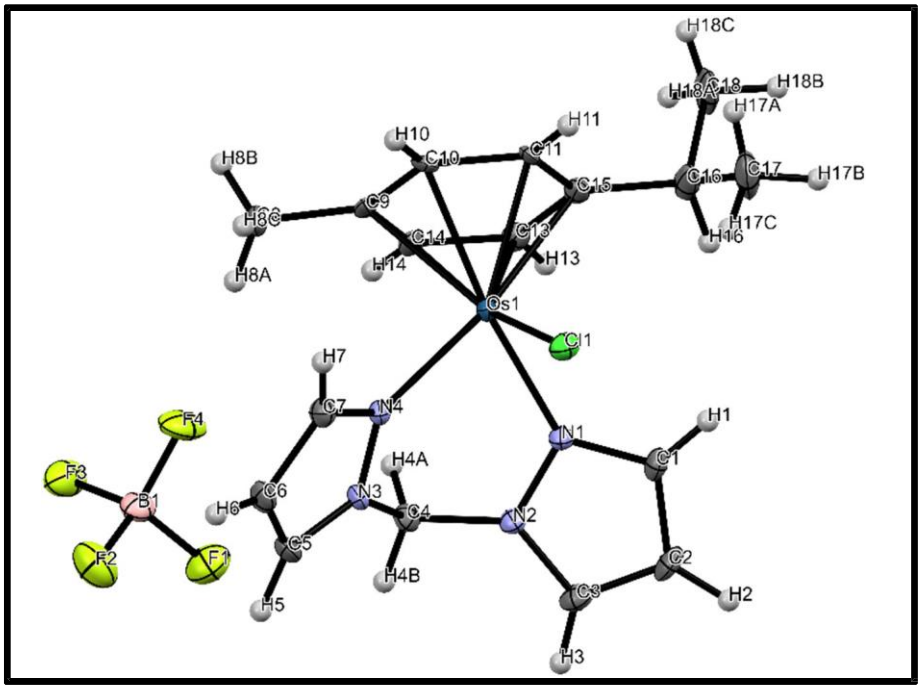

Figure 1. The Ortep diagram of **1** ($C_{17}H_{22}BClF_4N_4Os$) showing its asymmetric unit. The thermal ellipsoids were drawn at the 50% probability level.

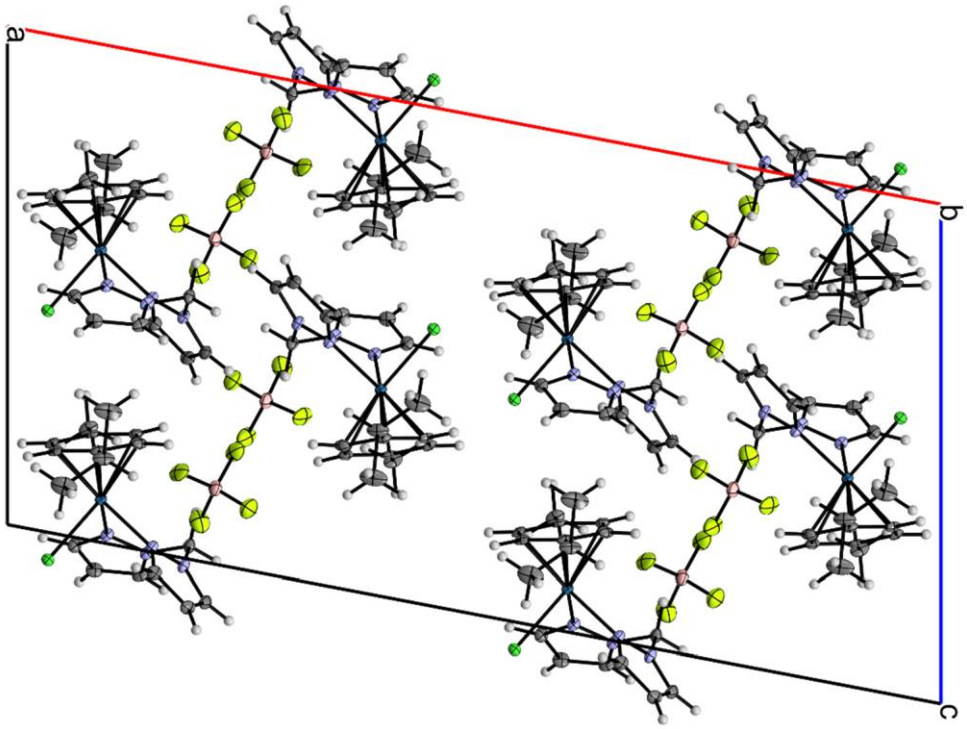

Figure 2. The unit cell and the packing of **1** ($C_{17}H_{22}BClF_4N_4Os$).

Table 1. Crystal data and structure refinement parameters for **1** ($C_{17}H_{22}BClF_4N_4Os$).

Identification code for 1	cu_am_ro_am_10_5_0m
Crystal (Colour /Shape)	Yellow /Block
Formula Weight	594.84
Temperature (K)	102.22
Crystal system	Monoclinic
Space group	C2/c
a (Å)	27.4619(7)
b (Å)	10.2573(3)
c (Å)	14.4399(4)
α (°)	90
β (°)	100.8160(10)
Γ (°)	90
Volume ($Å^3$)	3995.24(19)
Z	8
$e_{calc,}$ g/cm^3	1.978
M (mm^{-1})	13.718
F(000)	2288
Crystal size (mm^3)	0.475 × 0.33 × 0.15
Radiation source, λ (Å)	Cu(K_α), 2 = 1.54178
2θ range for data collection (°)	6.554 to 136.734
Index ranges	$-32 \le h \le 32, -12 \le k \le 12, -17 \le l \le 16$
Reflections collected	17267
Independent reflections	3581 [R_{int} = 0.0446, R_σ = 0.0383]
Data/restraints/parameters	3581/0/256
Goodness-of-fit on F^2	1.245
Final R indexes [I ≥ 2σ(I)]	R_1 = 0.0275, wR_2 = 0.0659
Final R indexes [all data]	R_1 = 0.0277, wR_2 = 0.0661
Largest diff. peak/hole / e $Å^{-3}$	0.70/−1.68

Table 2. Selected bond length (Å) and angles (°) of **1** ($C_{17}H_{22}BClF_4N_4Os$).

Length, (Å)	
Os1-Cl1	2.3982(8)
Os1-N1	2.122(3)
Os1-N4	2.105(3)
Angles/°	
N4-Os1-Cl1	84.71(9)
N4-Os1-N1	83.17(11)
N1-Os1-Cl1	83.84(9)

3. Discussion

Evaluative studies on the potential of half-sandwich arene Os(II) complexes as anticancer metallodrugs have appeared in the literature [10–12]. This has motivated us to explore this aspect. However, there remain fewer reports of arene Os(II) with the flexible *N, N*-chelates, apart from those reported recently in references [13–15] on the Ru(II) analogues.

The FTIR spectrum of **1** (see Figure S1) shows the stretching and compression bands synonymous with functional groups in the free dpzm and *p*-cym ligands. However, there are distinctive shifts (relative to the free ligand) in the vibration frequencies of some of the bonds of **1**, especially those of the dpzm which are also in proximity to the N1/$4_{(donor)}$—Os coordination bonds. This indirectly confirms the coordination of the dpzm on the Os(II) metal ion. The shifts in the vibrational resonances are, however, less prominent on the bonds of the functional groups of the *p*-cym ligand. This may be due to efficient charge dispersal via delocalization within the arene ring such that its substituent, being also remotely located relative to the $C_{(\pi\ =\ donor)}$—Os coordination bonds, vibrates at frequencies that are also

most similar to those of the free ligand. Additionally, there is a sharp absorption band at 1037.62 cm^{-1} due to the vibronic stretch of the bond of the BF_4^- counter ion.

The UV-Visible absorption spectrum (see Figure S2) shows a strong absorption band below 300 nm and shoulder below 350 nm due to the strong π–π* and n–π* electron transitions, respectively. There is also a weak and broad band between 350 nm and 500 nm due to the weak metal-to-ligand charge transfer (MLCT) absorption band, which is characteristic of arene Ru/Os(II) complexes.

In the ^{1}H NMR spectrum (see Figure S3), the expected chemical shifts, the hyperfine splitting patterns and integrals of the distinctive protons of the dpzm and the *p*-cym ligands are all observed. As expected, the protons of **1** resonate at relatively deshielded chemical shifts (compared to the free ligand). This is in line with the σ/π-donation of the coordinated ligands towards the Os(II) ion. However, there is an orbit-spin (SO) shielding effect on the protons of the arene ligands due to the heavy atom (Os) effect of the Os(II) ion that shields the electron density of the donor atoms of the ligand. More indicative of the coordination of the dpzm are the distinctive resonances of the geminal methylene protons of the two arms of the dpzm ligand. They appear as pairs of doublet signals at $\delta_{(ppm)}$ values of 7.12 (*d*) and 6.05 (*d*), which is typical of the A(B)X spin system. The restricted fluxionality of the protons renders diastereotopicity in the conformations of the complex due to the inequivalence imposed on the -CH_2- protons of the bridging arms of dpzm upon its coordination to the Os(II) ion, which is observable in the timescale of the ^{1}H NMR experiment. The diastereotopicity of the bridging -CH_2-protons has been observed for the proton resonances of other isostructural and multidentate ligands with methylene spacer groups [16]. The η^6-*p*-cym protons give rise to two different sets of resonances at $\delta_{(ppm)}$ values of 6.33 and 6.23 due to their XA(A')—XB(B') spin systems.

When a solution of **1** (3 mg in 30 mL of methanol which had been modified with 0.1% formic/formate buffer as a protonation-aiding agent) was electrosprayed with the voltage of the sprayer needle set at about +2.2 kV, ions with *m*/*z* values of 509 amu (100%) due to the $[C_{17}H_{22}ClN_4Os]^+$ ions of **1** were detected (see Figure S4). The purity of the crystalline blocks of **1** was confirmed by elementary analysis, for which there was a good agreement between the theoretical and the experimental data; see the elementary data listed in the experimental section.

The crystal blocks of **1** ($C_{17}H_{22}BClF_4N_4Os$) were further analysed by single-crystal X-ray diffraction analysis, and details are given in the experimental section. The asymmetric unit of **1** (see Figure 1 for a perspective) comprises an [Os(II)(dpzm(η^6-*p*-cym)Cl]$^+$ cation and a tetraborate as an anion. The cation is formed by the η^6–π-coordination of a *p*-cym and two N and Cl donor atoms to an Os(II) ion, leading to the pseudo-octahedral "three-leg piano stool" geometry [10–15,17]. For this geometry, the η^6-*p*-cym constitutes the pseudo 'seat' of the stool and is π-bonded to Os(II) at the Os–C bond distances (Os1—(C9, C10, C15) ranging from 2.161(4) to 2.214(4) Å, making a centroid (*p*-cym ring-Os1) distance of 1.671 Å. The metal centre is σ-bonded to the flexible dpzm chelate at asymmetric bond distances of 2.122(3) Å (Os1—N1) and 2.105(3) Å (Os1—N4). The chlorido co-ligand is bonded at a distance of 2.3982(9) Å (Os1—Cl1). These bond distances are close to those reported for related Os(II) complexes [10,18]. The N1, N4 and Cl1 donor atoms are staggered relative to the carbon atoms of the cymene and form the pseudo legs of the piano-stool structure. The bond angles (∠s) are typical of octahedral half-sandwiches bearing a flexible N, N-bidentate chelates and are 83.83(9)° (∠N1—Os1—Cl1), 83.17(12) (∠N1—Os1—N4) and 84.71(9)° (∠ N4—Os1—Cl1). They do not differ by more than 8° from 90° for an ideal octahedral geometry. However, the flexibility foisted by the methylene carbon of the chelate makes the N1—Os1—N4 angle significantly larger compared to other complexes chelated by rigid and aromatic N, N-ligands. All C—C, C—N and B—F bond lengths and associated angles are in the expected ranges for N, N/*O*-chelated *p*-cym ring Os(II) complexes [18].

When viewed along the *b*-axis (see Figures 2 and 3), the cations of **1** are packed as complementary columnal duets along the *c*-axis and are stabilized by Cl1 H1.—

C (2.640 Å) short contacts. As shown in Figure 3, these dimeric stacks are bridged by tetra-furcated short-range interactions involving the fluorine and boron atoms of the tetraborate anions as hydrogen bond donors and acceptors, respectively. The quadruped and short range-interactions are the F1 . . . ..H13—C13 (2.636Å); F3 H14—C13 (2.481Å); F4 . . . ..H8—C8 (2.235 Å) and C5 (π edge) B1 (3.574 Å). Numerous other short contacts further stabilized these cationic columns into a stable 3D structure.

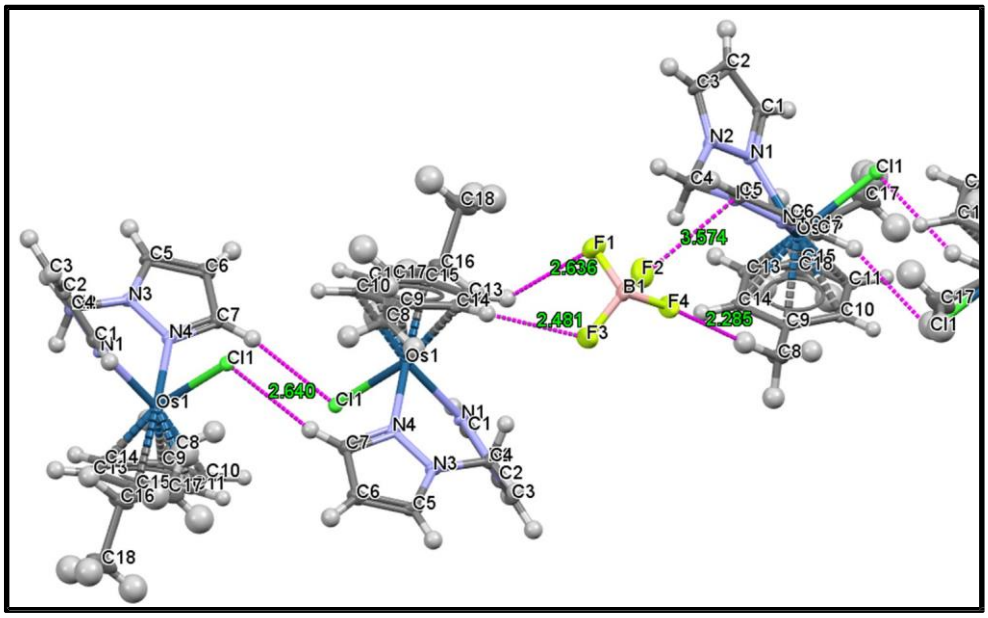

Figure 3. A view along the *b*-axis, showing the 1D-short contacts which support the columnar stacking of dimers of **1** ($C_{17}H_{22}BClF_4N_4Os$) (projecting along the *ab*-plane).

4. Materials and Methods

4.1. Synthetic Procedure for ***1***

Compound **1** was synthesized under an inert atmosphere of N_2 gas using the Schlenk techniques [19]. A solution of $[(\eta^6\text{-}p\text{-cym})Os(\mu\text{-Cl})(Cl)]_2$ (100 mg, 0.1265 mmol in 10 mL acetonitrile) was added in drops to a solution of dpzm (2.2 mmol in 5 mL acetonitrile) over 30 min. The mixtures were stirred for 4 h at 40 °C (Scheme 1) The unreacted material was filtered off and the filtrate concentrated to about 2 mL. About 1 mL of an ethanolic solution of NH_4BF_4 (saturated) was slowly added to the mixture and further stirred for 1 h in the dark under a cooling bath of ice. The yellow precipitate was filtered and washed with cold diethyl ether and dried under vacuum. Crystal blocks for X-ray diffraction analysis were grown by slow evaporation from the methanol solutions of the powder.

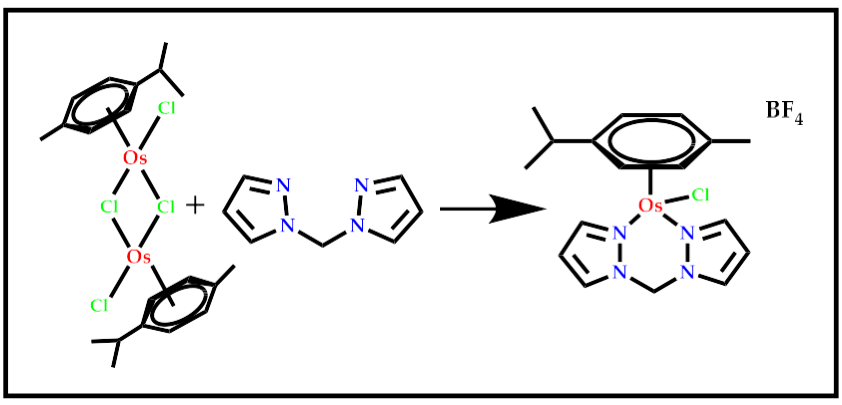

Scheme 1. Synthetic route for **1**. Reagents and conditions; MeOH/ EtOH, 40 °C, N_2 flow, 4 h and subsequent precipitation with NH_4BF_4.

4.2. Spectroscopic Characterization of 1

Compound **1** was characterized by several spectroscopic techniques. The NMR spectrum was recorded on a Bruker Avance 300 MHz spectrometer in DMSO-*d6* with residual signals of the solvent as the internal standard at ambient temperature. Chemical shifts were reported in ppm δ units. Coupling constants (*J*) were calculated in Hertz (Hz.). Mass spectral data were acquired on a Shimadzu LC-MS 2020 Spectrometer. Elemental composition analysis was performed on Thermal Scientific Flash 2000 CHN combustion analyzer. The UV-visible absorption spectrum was acquired using Carry 100 Bio UV-visible spectrophotometer. The infrared spectrum was recorded using a PerkinElmer Spectrum 100 FT-IR spectrometer (Waltham, MA, USA). Yield 67.5 %, yellow crystal blocks, ^{1}H NMR (300 MHz, DMSO-d_6) δ (ppm), 8.16 (*d*, *J* = 2.1 Hz, $2H_{(pzn)}$, 7.91 (*d*, *J* = 2.1, $2H'_{(pzn)}$, 7.12 (*d*, *J* = 14.4 Hz, $1H_{(pzn)}$, 6.65 (*t*, *J* = 2.6 Hz, $2H_{(pzn)}$, 6.33 and 6.23 (*d*, *J* = 5.6 Hz, 5.7 Hz, $4H_{(\eta6\text{-}p\text{-cym.})}$, 6.05 (*d*, *J* = 14.4 Hz, $1H_{(pzn)}$, 2.73 (*septet*, *J* = 6.9 Hz, $1H_{(\eta6\text{-}p\text{-cym's -CH(isopropyl)}}$, 2.05 (*s*, $3H_{(\text{methyl grp. of } \eta6\text{-}p\text{-cym})}$, 1.21 (*d*, *J* = 6.9 Hz, $6H_{(\eta6\text{-}p\text{-cym's two methyl grps. of the isopropyl})}$. FTIR (KBr, *υ*, cm^{-1}, w/m/s = weak/medium/strong intensity, shp/br =sharp/broad); $3132_{(w,\ Carom\text{-}H)}$, $2945_{(w,\ CH2methylene)}$, $1516_{(m,\ (C=N)}$, $1408_{(m.\ C=C)}$, $1281_{(m,\ \beta(c=c)\text{-}CH)}$, $1038_{(s,\ br\ BF4\text{-})}$, $830_{(m,\ shp,\ Os\text{-}N)}$ and $620_{(m,\ shp,\ Os\text{-}Cl)}$. Elementary analysis: *Calculated for* $C_{17}H_{22}BClF_4N_4Os$, %: C 34.30; %H, 3.75; N, 9.42; *found,* % C, 33.98; H, 3.85; N, 9.14. MS *(ESI)*$^{+}$ *m/z* = 509 (100%) for pseudo molecular ion, $[C_{17}H_{22}ClN_4Os + 2HJ]^{+}{}_{(g)}$.

4.3. X-ray Diffraction Analysis of 1

Single crystal X-ray crystallographic data of **1** were collected on a Bruker APEX Duo [20,21] CCD area detector diffractometer with an Incoatec microsource operating at 30 W of power. The crystal was kept at 100.15 K during data collection using an Oxford Instruments Cryojet accessory. Diffraction was by graphite-monochromated Cu(K_α), *2* = 1.54178), at a crystal-to-detector distance of 50 mm. Data collection was performed at the following set conditions: ω-/φ-scans with exposures taken at 30 W X-ray power and 0.50 frame widths using SAINTS' APEX2 [22]. The crystal structure was solved with Olex2 [20], while the SHELXS [23] and SHELX [24] programs were used for structural refinement via direct methods. The non-hydrogen atoms were refined anisotropically by full-matrix least-squares minimization/refinement of F^2. Hydrogen atoms were included but not refined. Visualization of the crystallographic data was done in WinGX [25] and Mercury *υ*.4.3 [26]. See Table 1 for alignment.

Crystal structure data: monoclinic crystal system, C2/c (*no.* 15) space group *a* = 27.4619(7) Å, *b* = 10.2573(3) Å, *c* = 14.4399(4) Å, β = 100.8160(10)°, *V* = 3995.24(19) $Å^3$, *Z* = 8, *T* = 102.22 K, $\mu_{(Cu\ (K\alpha)}$ = 13.718 mm^{-1}, D_{calc} = 1.978 g/cm^3, $17267_{(reflections\ measured)}$ ($6.554° \leq 2\theta \leq 136.734°$), $3581_{(unique)}$ (R_{int} = 0.0446, R_σ = 0.0383), $R_{1(final)}$ = 0.0275 ($I > 2\sigma_{(I)}$), wR_2 = $0.0661_{(all\ data)}$.

5. Conclusions

$C_{17}H_{22}BClF_4N_4Os$ (1), an [Os(II)(dpzm(η^6-*p*-cym)Cl] tetrafluoroborate salt, was synthesised and characterized by several spectroscopic techniques. The slow evaporation of its methanolic solution afforded yellow crystal blocks of **1**, of good quality, for the single X-ray diffraction analysis. The title compound crystallizes in the monoclinic crystal system and in the C2/c (*no.* 15) space group. Its crystal structure adopts the pseudo-octahedral "three-leg piano stool" geometry, as widely reported for other arene Ru(II)/Os(II) complexes. The bond distances and angles are comparable to those reported for other analogous arene Ru(II)/Os(II) complexes [10].

Supplementary Materials: Figure S1: FTIR spectrum of **1**; Figure S2: UV-Visible absorption spectrum of **1**; Figure S3: ^{1}H NMR spectrum of **1**; Figure S4: Low-resolution ESI^{+} mass spectrum of **1**. Table S1: Atomic coordinates ($\times 10^4$) and equivalent isotropic displacement parameters ($Å^2 \times 10^3$) for **l1_sq** (**1**); Tables S2 and S3: Bond lengths [Å] and angles [°] for **l1_sq** (**1**), respectively.

Author Contributions: A.K.K.: investigation, conceptualization, synthesis, drafting; P.O.: conceptualization, partial resourcing supervision; J.G.: partial resourcing on synthesis, reviewing; R.O.O.: crystallization and spectral characterization, A.M.: X-ray diffraction data handling, data visualization and analysis, drafting and reviewing, partial resourcing. All authors have read and agreed to the published version of the manuscript.

Funding: This research received no external funding.

Institutional Review Board Statement: Not applicable.

Informed Consent Statement: Not applicable.

Data Availability Statement: CDCC No: 2164335 (**cu_am_ro_am_10_5_0m**) contains the supplementary crystallographic data for **1**. The data can be obtained free of charge via http://www.ccdc.cam.ac.uk/conts/retrieving.html (accessed on 4 April 2022), or from the Cambridge Crystallographic Data Centre, 12 Union Road, Cambridge CB2 1EZ, UK; fax: (+44)1223-336-033; or via email: deposit@ccdc.cam.ac.uk.

Acknowledgments: The Egerton University, Kenya is thanked for funding this work. Conceptualization and synthesis of the complex were carried out in the Department of Chemistry, Egerton University, Kenya. The University of KwaZulu-Natal, RSA is acknowledged for partial funding of this work. The crystallization and single-crystal X-ray diffraction analysis were performed in the School of Chemistry and Physics, PMB Campus, University of KwaZulu-Natal, RSA.

Conflicts of Interest: No potential conflicts of interest or competing interests are foreseen.

Sample Availability: Sample of the compound is available from the authors.

References

1. Nahari, G.; Tshuva, E.Y. Synthesis of asymmetrical diaminobis (alkoxo)-bisphenol compounds and their C1-symmetrical monoligated titanium(IV) complexes as highly stable highly active antitumor compounds. *Dalton Trans.* **2021**, *50*, 6423–6426. [CrossRef] [PubMed]
2. Sze, J.H.; Raninga, P.V.; Nakamura, K.; Casey, M.; Khanna, K.K.; Berners-Price, S.J.; Di Trapani, G.; Tonissen, K.F. Anticancer activity of a Gold(I) phosphine thioredoxin reductase inhibitor in multiple myeloma. *Redox Biol.* **2020**, *28*, 101310–101321. [CrossRef] [PubMed]
3. Nabiyeva, T.; Marschner, C.; Blom, B. Synthesis, structure and anti-cancer activity of osmium complexes bearing π-bound arene substituents and phosphane Co-Ligands: A review. *Eur. J. Med. Chem.* **2020**, *201*, 112483–112498. [CrossRef] [PubMed]
4. Wani, W.A.; Baig, U.; Shreaz, S.; Shiekh, R.A.; Iqbal, P.F.; Jameel, E.; Ahmad, A.; Mohd-Setapar, S.H.; Mushtaque, M.; Hun, L.T. Recent advances in iron complexes as potential anticancer agents. *New J. Chem.* **2016**, *40*, 1063–1090. [CrossRef]
5. Simovic´, A.R.; Masnikosa, R.; Bratsos, I.; Alessio, E. Chemistry and reactivity of ruthenium(II) complexes: DNA/protein binding mode and anticancer activity are related to the complex structure. *Coord. Chem. Rev.* **2019**, *398*, 113011–113036. [CrossRef]
6. Hanif, M.; Babak, M.V.; Hartinger, C.G. Development of anticancer agents: Wizardry with osmium. *Drug Discov. Today* **2014**, *19*, 1640–1648. [CrossRef] [PubMed]
7. Peacock, A.F.; Sadler, P.J. Medicinal organometallic chemistry: Designing metal arene complexes as anticancer agents. *Chem. Asian J.* **2008**, *3*, 1890–1899. [CrossRef] [PubMed]
8. Zhang, P.; Huang, H. Future potential of osmium complexes as anticancer drug candidates, photosensitizers and organelle-targeted probes. *Dalton Trans.* **2018**, *47*, 14841–14854. [CrossRef]
9. Allardyce, C.S.; Dyson, P.J. Ruthenium in medicine: Current clinical uses and future prospects. *Platinum Met. Rev.* **2001**, *45*, 62–69.
10. Păunescu, E.; Nowak-Sliwinska, P.; Clavel, C.M.; Scopelliti, R.; Griffioen, A.W.; Dyson, P.J. Anticancer Organometallic Osmium(II)-*p*-cymene Complexes. *ChemMedChem* **2015**, *10*, 1539–1547. [CrossRef] [PubMed]
11. Peacock, A.F.; Habtemariam, A.; Moggach, S.A.; Prescimone, A.; Parsons, S.; Sadler, P.J. Chloro half-sandwich osmium(II) complexes: Influence of chelated N, N-ligands on hydrolysis, guanine binding, and cytotoxicity. *Inorg. Chem.* **2007**, *46*, 4049–4059. [CrossRef] [PubMed]
12. van Rijt, S.H.; Peacock, A.F.; Johnstone, R.D.; Parsons, S.; Sadler, P.J. Organometallic osmium (II) arene anticancer complexes containing picolinate derivatives. *Inorg. Chem.* **2009**, *48*, 1753–1762. [CrossRef] [PubMed]
13. Gichumbi, J.M.; Omondi, B.; Friedrich, H.B. Crystal structure of η⁶-p-cymene-iodido-(N-isopropyl-1-(pyridin-2-yl)methanimine-κ²N,N′)ruthenium(II) hexafluorophosphate(V),) $C_{19}H_{26}IN_2F_6Ru$. *Z. Krist. New Cryst. Struct.* **2020**, *235*, 485–487. [CrossRef]
14. Thangavel, S.; Rajamanikandan, R.; Friedrich, H.B.; Ilanchelian, M.; Omondi, B. Binding interaction, conformational change, and molecular docking study of N-(pyridin-2-ylmethylene) aniline derivatives and carbazole Ru (II) complexes with human serum albumins. *Polyhedron* **2016**, *107*, 124–135. [CrossRef]

15. Gichumbi, J.M.; Omondi, B.; Friedrich, H.B. Crystal structure of (η⁶-1-isopropyl-4-methyl benzene)-(N-(2,5-dichlorophenyl)- 1-(pyridin-2-yl)methanimine-k²N,N′)ruthenium(II) perchlorate, $C_{22}H_{22}Cl_4N_2O_4Ru$. *Z. Kristallogr. NCS* **2018**, *233*, 423–425. [CrossRef]
16. Marchetti, F.; Pettinari, C.; Pettinari, R.; Cerquetella, A.; Di Nicola, C.; Macchioni, A.; Zuccaccia, D.; Monari, M.; Piccinelli, F. Synthesis and intramolecular and interionic structural characterization of half-sandwich (arene) ruthenium(II) derivatives of bis (pyrazolyl) alkanes. *Inorg. Chem.* **2008**, *47*, 11593–11603. [CrossRef]
17. Gichumbi, J.M.; Friedrich, H.B.; Omondi, B. Crystal structure of chlorido-(η⁶–1-isopropyl-4-methylbenzene)-(1-(pyridin-2-yl)-N- (p-tolyl)methanimine-κ²N,N′)tuthenium(II) hexafluorophosphate(V) $C_{23}H_{26}ClF_6N_2PRu$. *Z. Krist. New Cryst. Struct.* **2017**, *232*, 285–287. [CrossRef]
18. Schreiber, D.F.; O'Connor, C.; Grave, C.; Müller-Bunz, H.; Scopelliti, R.; Dyson, P.J.; Phillips, A.D. Synthesis, Characterization, and Reactivity of the First Osmium β-Diketiminato Complexes and Application in Catalysis. *Organometallics* **2013**, *32*, 7345–7356. [CrossRef]
19. Gichumbi, J.M.; Friedrich, H.B.; Omondi, B.; Naicker, K.; Singh, M.; Chenia, H.Y. Synthesis, characterization, antiproliferative, and antimicrobial activity of osmium(II) half-sandwich complexes. *J. Coord. Chem.* **2018**, *71*, 342–354. [CrossRef]
20. Dolomanov, O.; Bourhis, L.; Gildea, R.; Howard, J.; Puschmann, H. OLEX2: A complete structure solution, refinement and analysis program. *J. Appl. Cryst.* **2009**, *42*, 339–341. [CrossRef]
21. CCD CrysAlis. *CrysAlis Red*; Xcalibur PX Software; Oxford Diffraction Ltd.: Abingdon, UK, 2008.
22. Bruker, A. *Saint and SADABS*; Bruker AXS Inc.: Madison, WI, USA, 2009.
23. Sheldrick, G.M. SHELXT–Integrated space-group and crystal-structure determination. *Acta Cryst.* **2015**, *71*, 3–8. [CrossRef] [PubMed]
24. Sheldrick, G.M. A short history of SHELX. *Acta Cryst.* **2008**, *64*, 112–122. [CrossRef] [PubMed]
25. Farrugia, L.J. WinGX and ORTEP for Windows: An update. *J. Appl. Crystallogr.* **2012**, *45*, 849–854. [CrossRef]
26. Macrae, C.F.; Bruno, I.J.; Chisholm, J.A.; Edgington, P.R.; McCabe, P.; Pidcock, E.; Rodriguez-Monge, L.; Taylor, R.; Streek, J.; Wood, P.A. Mercury CSD 2.0–new features for the visualization and investigation of crystal structures. *J. Appl. Crystallogr.* **2008**, *41*, 466–470. [CrossRef]